View Article Online / Journal Homepage / Table of Contents for this issue

A reversible switch for hydrogen adsorption and desorption: electric fields†

W. Liu,[ab] Y. H. Zhao,[b] Y. Li,[b] E. J. Lavernia*[b] and Q. Jiang*[a]

Received 15th April 2009, Accepted 23rd July 2009
First published as an Advance Article on the web 17th August 2009
DOI: 10.1039/b907591g

Published on 17 August 2009. Downloaded on 7/6/2022 4:08:17 AM.

Implementation of hydrogen storage systems requires moderate bonding strength. However, this goal has remained a challenge, either due to the weak physisorption or extremely strong chemisorption. Here, we report on a new phenomenon, namely that H_2 binding can be externally enhanced (or weakened) *via* superimposition of a positive (or negative) electric field. We demonstrate this concept using an 8-Li-doped carbon nanotube. The calculated adsorption energy $E_{ad} = -0.58$ eV/H_2 under $F = +0.010$ au is 93.33% lower than that under 0.000 au (F indicates the field intensity). This is because the positive field produces an extra dipole moment. In contrast, E_{ad} increases from −0.30 to −0.20 eV/H_2 when $F = -0.010$ au. In view of the fact that storage systems are insensitive to small unexpected field fluctuations, the application of the electric field as a reversible switch makes practical sense.

Introduction

Nanostructured materials have emerged as potential candidates for hydrogen storage, given their high surface to volume ratios and diverse physical properties.[1–4] For practical applications, a moderate binding strength in the range of $-0.70 \leq E_{ad} \leq -0.20$ eV/H_2 was suggested at room temperature, where E_{ad} is the adsorption energy between the H_2 molecules and the storage media.[5,6] This presents a quandary, since on one hand this requires enhancing the weak binding between the H_2 and solid surfaces, which results from the strong H–H bond and the closed-shell electronic configuration.[7] On the other hand, an excessively strong bond is not ideal either since ultimately both storage and desorption of H_2 are necessary.[8]

Inspection of the published literature shows that H_2 is either chemisorbed in the atomic form or physisorbed in the molecular form. Carbon nanostructures, including single-wall carbon nanotubes (SWCN),[9–14] C_{60} fullerene,[8,15,16] and graphene,[10,17] are the most common storage media. In addition, other storage media such as metal organic frameworks (MOFs)[18,19] and covalent organic frameworks (COFs)[20] have also been studied for hydrogen storage in recent years. Their storage abilities can be largely improved *via* metal doping, due to the enhanced charge transfer from metal to carbon.[10] Noteably, although the alkali[8–10,12,13,21] and transition metals[6,17,22,23] are often utilized as dopants, a recent work predicted that Ca is the most attractive metal for functionalizing fullerenes.[24] In comparison with carbon-based nanostructures, the TiB_2,[25] WC,[26] and BN[7,23] nanotubes were proven to be better storage materials. This is because their inner heteropolar bonding, such as the ionic B–N in BN, is beneficial to the H_2 straoge.[7] Moreover, it was reported that H_2 binding on the cation Li (Li^+) is much stronger than on the neutral Li-doped nanotube.[27] This behavior is derived from the fact that the bonding of H_2 with the neutral Li is covalent, whereas that with Li^+ is primarily caused by polarization.

It is evident from the above discussion that the binding will be increased if the ionization can be further enhanced; hence, storage materials tend to be complex, and impractical. We propose the introduction of electric fields into hydrogen storage models, because the fields are readily imposed and they have been proven to be an effective approach to redistribute charges.[28–31] In fact, a very recent paper has computationally studied the electric field enhanced hydrogen adsorption phenomenon on nano-scale BN sheet, where the calculated E_{ad} value drops dramatically from −0.07 to −0.48 eV/H_2 in the presence of a 0.050 au field.[32] In our recent published work, an 8-Li-doped (8,0) SWCN (the Li_8/SWCN system) has been established as a hydrogen storage media.[33] Our calculations demonstrated that, at most, 64 H_2 molecules can be adsorbed which renders a high gravimetric density of 13.45 wt %. Therefore, the multiple Li doped carbon nanotube is still employed as a model material to look into the influence of electric fields on H_2 binding strength in this work. Although field enhanced hydrogen adsorption has been studied on BN sheets, the superimposition of electric fields to metal-decorated carbon nanotubes has heretofore never been reported for hydrogen storage. Notable is the fact that most previous studies addressed the problem of bonding enhancement but failed to address the problem of how to decrease the binding during the desorption process. In fact, one can hypothesize that the binding will weaken if the charges transfer in a contrary direction, *i.e.*, from the nanostructures to the

[a] *Key Laboratory of Automobile Materials, Ministry of Education, and School of Materials Science and Engineering, Jilin University, Changchun, 130022, China. E-mail: jiangq@jlu.edu.cn; Fax: +86 (0)431 85095876; Tel: +86 (0)431 85095371*
[b] *Department of Chemical Engineering and Materials Science, University of California, Davis, CA 95616, United States. E-mail: lavernia@ucdavis.edu; Fax: +1 (1)530 752 8058; Tel: +1 (1)530 752 0554*

† Electronic supplementary information (ESI) available: Atomic coordinates and absolute energies of all optimized structures. See DOI: 10.1039/b907591g

View Article Online

Published on 17 August 2009. Downloaded on 7/6/2022 4:08:17 AM.

dopants. In this study we propose that this can be readily accomplished by simply changing the direction of the superimposed electric fields.

In this contribution, several electric fields with different directions and intensities are applied to the relaxed Li_8/SWCN storage materials. The adsorption structures are determined in terms of their corresponding E_{ad} values. The electronic analyses are employed to investigate the binding mechanism. The results of H_2 on the 8-Li-doped SWCN are compared with those corresponding to pure and 1-Li-doped SWCNs.

Computational framework

Density functional theory (DFT) calculations were performed with the DMol^3 code.[34,35] Li has an odd number of electrons, in the entire system the number of spin-up and spin-down electrons will not be equal, and thus the unrestricted spin-polarized option is chosen during the entire calculation. Despite the fact that it generally overestimates the H_2 binding strength, the local density approximation (LDA) function is both reliable and computationally efficient and hence it is often used for the study of systems involving the van der Waals interactions.[36–38] In particular, LDA has been proven to be suitable for atoms with very few electrons (such as H, Li, and C),[39–41] and even for charged carbon nanostructures with ions and electric fields.[41,42] In view of the fact that both light elements and electric fields are involved in our system, it is appropriate to invoke LDA with the Perdew–Wang correlation (PWC)[43] functional throughout the paper. An additional argument that compelled our selection of the LDA approach instead of the generalized gradient approximation (GGA) is that electric field calculations are quite time-consuming, especially for our relatively large system with 74 atoms. In this study, we adopted all-electron calculations with double numeric plus polarization (DNP) basis sets implemented in the DMol^3 code.[34] Since in our systems the band gap between the highest occupied molecular orbital (HOMO) and lowest unoccupied molecular orbital (LUMO) is small and there are significant occupied states in the vicinity of the Fermi level, the technique of smearing was applied to the orbital occupation to speed up self-consistent field (SCF) convergence.[44] Since the obtained results are very sensitive to the accuracy settings under the electric fields, the smearing was set to 0.002 Ha, the real-space global orbital cutoff radius was chosen to be as high as 6.0 Å, and k-points was $1 \times 1 \times 8$.

The adsorption energy E_{ad} is defined as the negative of the value obtained by subtracting the total energy of the fragments (Li_m/SWCN and H_2) from the adsorbed system (H_2/Li_m/SWCN) at the equilibrium geometry. The $E_{ad}(F)$ values are indicative of the energy obtained under the intensity of field F. In this case, the energy of the fragments should also be obtained in presence of the external F.[45] Thus,

$$E_{ad}(F) = E_F(H_2/Li_m/SWCN) - E_F(Li_m/SWCN) - E_F(H_2), \quad (1)$$

where the subscript "m" indicates the numbers of Li atoms. H_2 is docked into the vacuum with an initial bond length $d_{H-H} = 0.74$ Å.[46] In view of the fact that our goal is to investigate the influence of electric fields on the H_2 binding strength, only one H_2 molecule is studied throughout the paper. The storage is primary physisorption with van der Waals forces in nature, and thus H_2 maintains its molecular identity.[47] The negative value of E_{ad} indicates that the adsorption is exothermic and hence stable.[48] When no external field is applied, $F = 0.000$ au in the above equation. Before calculating the eight Li doped model, the small H_2/Li/SWCN system is chosen as a prototype to check the validity of our calculations. After relaxation, $E_{ad} = -0.24$ eV, $d_{H-H} = 0.77$ Å, and $d_{Li-H} = 1.96$ Å listed in Table 1 are very close to other LDA simulation results with $E_{ad} = -0.26$ eV, $d_{H-H} = 0.78$ Å, and $d_{Li-H} = 1.98$ Å.[12] Since the E_{ad} value only reflects the stability of the H_2 molecule on the Li-doped nanotubes, we selected the H_2/Li/SWCN as a model system to determine the energy barrier for this reaction. Our results showed that the adsorption of hydrogen occurs spontaneously without an energy barrier, which is consistent with previous findings that no energy barrier has to be overcome when a H_2 is adsorbed by a Ti-decorated nanotube or a fullerene.[22,49]

To investigate the variations of H_2 binding induced by the external electric fields, a storage model composed of Li doped (8,0) SWCN was established for this simulation. As shown in Fig. 1, four lines of Li atoms dispersed symmetrically at the hollow positions above the hexagonal rings, and the length of the tube equals to twice of the periodicity of the (8,0) SWCN, where the z direction was taken to be along the axis of SWCN. Thus, eight Li and sixty-four C atoms exist within the smallest unit cell in total. Notable is the fact that this Li_8C_{64} model represents a special configuration that strictly obeys the arrangement rules for high coverage metals: if one carbon hexagon has one dopant, all the neighboring ones do not.[9,50,51] This arrangement ensures both the large distances between the

Table 1 Electric field induced E_{ad} values in eV/H_2, and geometric parameters in Å (atomic distance d, and diameters Ø of the nanotubes) for the stable configurations for the H_2/Li_8/SWCN, H_2/Li/SWCN, and H_2/SWCN systems. The atomic coordinates and absolute energies of optimized structures are provided in the ESI[fn1]†

System	Site	F	$-E_{ad}$	d_{Li-H}	d_{Li-C}	d_{H-H}	$Ø_x$[c]	$Ø_y$[c]
		+0.010	0.58[a]	1.80	1.56	0.78	6.55	6.13
	Bridge	0.000	0.30	1.91	1.49	0.79	6.36	6.35
		−0.010	0.20	1.99	1.62	0.78	8.27	4.33
		+0.010	0.56	1.95	1.56	0.79	6.43	6.15
H_2/Li_8/SWCN	Middle	0.000	0.25	1.98	1.51	0.80	6.38	6.33
		−0.010	0.11	2.09	1.61	0.78	8.21	4.41
		+0.010	0.16	1.98	1.54	0.77	6.50	6.14
	Atop	0.000	0.15	1.98	1.51	0.78	6.37	6.35
		−0.010	0.10	1.99	1.62	0.77	8.28	4.31
H_2/Li/SWCN	Bridge	+0.010	0.24[b]	1.98	1.61	0.78	6.47	6.14
		0.000	0.24	1.96	1.59	0.77	6.17	6.47
H_2/SWCN	Atop	+0.010	0.10	—	—	0.77	6.58	5.97
		0.000	0.10	—	—	0.77	6.31	6.32

[a] Convergence tests were done for this structure, where $E_{ad} = -0.67$ eV when k-points and cutoff radius are $1 \times 1 \times 5$ and 4.4 Å, respectively; $E_{ad} = -0.55$ eV when settings increase to $1 \times 1 \times 8$ and 5.5 Å; $E_{ad} = -0.58$ eV when settings increase to $1 \times 1 \times 8$ and 6.0 Å; $E_{ad} = -0.55$ eV when $1 \times 1 \times 9$ and 7.0 Å. All smearing values are 0.002 Ha. [b] E_{ad} is still −0.24 eV when the accuracy settings are increased to $k = 1 \times 1 \times 9$, and cutoff is 7.0 Å. [c] The subscripts "x" and "y" indicate the diameter values along the horizontal and vertical directions.

 This journal is © the Owner Societies 2009

View Article Online

Published on 17 August 2009. Downloaded on 7/6/2022 4:08:17 AM.

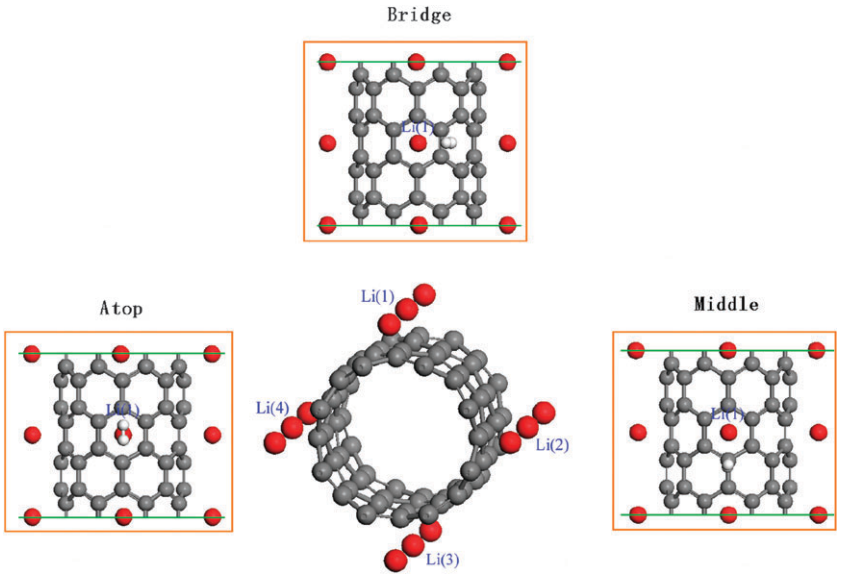

Fig. 1 A schematic plot for the Li_8/SWCN storage material. The three insets show the possible adsorption sites of a H_2 molecule on this model. The red, gray, and white spheres represent Li, C, and H atoms, respectively. Note that the H–H bond is vertical to the nanotube at the Middle site, and thus only one H can be seen from the top view.

neighboring metals and the equilibrium of the entire system. Otherwise, the metals delocalize from the center of the hollow sites and intend to aggregate into a cluster when all the neighboring six hexagonal rings are occupied by Li. In fact, the concentration of Li : C = 1 : 8 in our model is far below the critical doping value of 1 : 3 required to avoid Li segregation on graphenes and nanotubes.[52] In contrast, too low of a concentration of metal dopants is not a good choice either, since in this case the carbon atoms cannot be fully ionized and the H_2 binding strength will be lowered. A cubic supercell of $20 \times 20 \times 8.52$ Å^3 is used to avoid the interactions from neighboring molecules. As shown in the insets of Fig. 1, three possible adsorption sites exist around a dopant: 1. Atop site (H_2 lies on top of a Li atom); 2. Bridge site (H_2 locates beside a Li atom and on top of a C–C bond); and 3. Middle site (H_2 locates between two neighboring Li atoms). Since the four lines of Li atoms are symmetrically placed on the carbon nanotube, the calculated result will not change when a H_2 adsorbs on different Li atoms. However, to consider a uniform arrangement the molecule is placed around the uppermost Li(1) atom, as seen in Fig. 1. Electric fields with $F = 0.010$ au are applied to all the storage models, in the upward (defined as a positive field) or downward (defined as a negative field) direction normal to the nanotube. In addition to the directions, a series of fields with F values between −0.010 and +0.010 au are also utilized to study the intensity dependence. The density of states (DOS) is determined to clarify the effect of Li-doping on the H_2 storage in SWCNs. For comparison purposes, similar calculations are also carried out for the pure SWCN (H_2/SWCN) and the 1-Li-doped SWCN (H_2/Li/SWCN), where the most stable site for the hydrogen storage is the Atop and Bridge site, respectively. The adsorption mechanisms are discussed in terms of the Mulliken population analysis, which can provide a clear and definitive description for charge redistribution, even in the presence of an electric field.[53,54]

Results and discussion

We first consider the results obtained in the absence of electric fields. For the relaxed Li_8/SWCN, the Li–C atomic distance $d_{Li–C} = 1.48$ Å with a relatively strong binding of 1.82 eV/atom. Charges transfer from the dopants to the SWCN in terms of the Mulliken analysis: Li presents a net charge of +0.291 e, while the neighboring C atoms present negative ones of −0.088 and −0.013 e. These results verify the stability of our 8-Li-doped models. The calculated E_{ad} values for a H_2 molecule on the Li_8/SWCN systems are listed in Table 1. After full relaxation, H_2 is parallel to SWCN at the Atop site with $E_{ad} = -0.15$ eV/H_2. In contrast, the H–H bonds tilt at the Bridge and Middle sites, whose corresponding E_{ad} values are −0.30 and −0.25 eV/H_2, respectively. Thus, the Bridge site is more preferable than the rest. This can be confirmed by the geometric parameters in this table, where the $d_{Li–H} = 1.91$ Å at the Bridge site is less than $d_{Li–H} = 1.98$ Å at the Middle and Atop sites. The storage materials expand slightly after H_2 is adsorbed in terms of the $d_{Li–C}$ values. The free H–H bond increases from 0.77 to 0.78–0.80 Å after adsorption, which is consistent with other simulation results.[12] As listed in Table 2, the net charge of a H_2 molecule increases from 0 to +0.128 e after adsorption, which implies that the interaction between the H_2 and the media involves both physisorption and chemisorption. Table 1 also provides the calculation results for the Atop site in the H_2/SWCN and the Bridge site in the H_2/Li/SWCN where $E_{ad} = -0.10$ and −0.24 eV/H_2, respectively. The latter is very close to literature datum of $E_{ad} = -0.26$ eV/H_2.[12] In addition, it is discernable that the binding strength can be enhanced by introducing more dopants. In our recent work, the average $E_{ad} = -0.20$ and −0.17 eV/H_2, respectively, when 32 and 64 H_2 molecules are adsorbed on the same Li_8/SWCN material.[33] Given that $E_{ad} = -0.30$ eV/H_2 when a single H_2 is studied, it is evident that the binding strength will be lowered when more molecules are stored by the material.

View Article Online

Table 2 The Mulliken charge analysis for the atoms before and after a H_2 molecule on the Bridge site in the Li_8/SWCN system under F = 0.000, +0.010, −0.010, +0.002, and −0.005 au, where the unit of the atom charge is one electron charge e

Structure	Atom	F = 0.000 au		F = +0.010 au		F = −0.010 au		F = +0.002 au		F = −0.005 au	
		Before	After	Before	After	Before	After	Before	After	Before	After
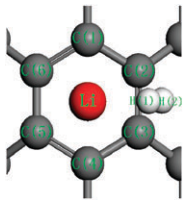	H(1)	0.000	−0.001	+0.087	+0.048	−0.087	+0.014	+0.018	+0.001	−0.044	+0.012
	H(2)	0.000	+0.129	−0.087	+0.139	+0.087	+0.142	−0.018	+0.128	+0.044	+0.134
	Li	+0.291	+0.151	+0.423	+0.203	+0.385	+0.242	+0.333	+0.177	+0.379	+0.205
	C(1)	−0.088	−0.079	−0.118	−0.108	+0.011	+0.011	−0.116	−0.102	−0.077	−0.064
	C(2)	−0.013	−0.027	−0.048	−0.050	+0.029	+0.033	−0.013	−0.023	+0.001	−0.003
	C(3)	−0.013	−0.024	−0.048	−0.056	+0.029	+0.035	−0.013	−0.025	+0.001	−0.002
	C(4)	−0.088	−0.081	−0.118	−0.105	+0.011	+0.013	−0.116	−0.101	−0.077	−0.065
	C(5)	−0.014	−0.022	−0.048	−0.052	+0.030	+0.021	−0.015	−0.020	+0.004	+0.001
	C(6)	−0.014	−0.022	−0.048	−0.047	+0.030	+0.022	−0.014	−0.020	+0.004	+0.001

Published on 17 August 2009. Downloaded on 7/6/2022 4:08:17 AM.

The similar trend has also been observed in the H_2/BN sheet, where E_{ad} = −0.07 eV for the single H_2, while increases to −0.03 eV/H_2 when a layer of H_2 molecules is adsorbed.[32]

Now, we address the effect of the electric fields on E_{ad} values for the H_2/Li_8/SWCN. From Table 1, E_{ad} values at the Bridge site decrease dramatically to −0.58 eV/H_2 under F = +0.010 au, where F indicates the field intensity. This is almost doubled in comparison with E_{ad} = −0.30 eV/H_2 at F = 0.000 au. Furthermore, it is even fivefold lower than E_{ad} = −0.10 eV/H_2 on a pure SWCN. The geometry of SWCN varies severely under the field, where $Ø_x$ increases from 6.36 to 6.55 Å and $Ø_y$ decreases from 6.35 to 6.13 Å. This renders the shape of the cross section to change from circular to elliptical. $d_{Li–H}$ decreases from 1.91 to 1.80 Å, which verifies the increase of the binding strength. In addition, $d_{Li–C}$ increases from 1.49 to 1.56 Å while $d_{H–H}$ decreases slightly. The question arises as to whether only the most stable Bridge site presents such phenomena. To examine this question, both the Middle and Atop sites are further calculated under F = +0.010 au. For the former, it is readily seen from Table 1 that the E_{ad} value also decreases significantly from −0.25 to −0.56 eV/H_2. This suggests that both the Bridge and the Middle are excellent storage sites since their corresponding E_{ad} values are similar. Nevertheless, only 0.01 eV/H_2 variation is obtained at the Atop site under the field.

When we observe $d_{Li–H}$ values from different sites, there is a sequence of Bridge < Middle < Atop, which is consistent with the sequence of their corresponding E_{ad} values. Thus, the binding strength between the H_2 and Li is inversely proportional to their corresponding d values, even though in the presence of fields. In contrast, the field seems to have no obvious contribution to the E_{ad} values for H_2/Li/SWCN and H_2/SWCN systems. This may be due to the weak spin variation around the nanotube induced by only one metallic atom or even lack of any metallic atom. In fact, only a 2.36% charge variation can be detected under fields for the Li atom in the Li/SWCN system.

To understand the reason why the binding can be enhanced under F = +0.010 au, the Mulliken charge analysis is carried out for the Bridge site, and the results around the dopant are listed in Table 2. On the one hand, the charge carried by each Li increases considerably from +0.291 to +0.423 e for the un-adsorbed system since the electrons will move downward from Li to the carbon ring under a positive field. On the other hand, the charges of the surrounding six C atoms decrease from −0.088 to −0.118 e, or from −0.014 to −0.048 e. Therefore, the positive field results in the enhancement of charge transfer from Li to C, *i.e.* further ionization,[10] which increases the H_2 sorption. After adsorption, the H_2 loses 0.187 e while Li obtains 0.220 e charges, whereas small changes can be found in C atoms.

Obviously, opposite binding trends might be achieved if the negative fields are employed. In Table 1, E_{ad} = −0.20, −0.11, and −0.10 eV/H_2 at Bridge, Middle, and Atop sites, respectively. Comparing with the data without fields, all the binding values are weakened under F = −0.010 au. All their $d_{Li–H}$ values increase after introducing the field, where $d_{Li–H}$ = 1.99 Å at the Bridge site. The SWCN is severely compressed along the direction of the field, where $Ø_x$ considerably increases from 6.36 to 8.27 Å and $Ø_y$ decreases from 6.35 to 4.33 Å. In terms of the charge analysis results in Table 2, it is interesting to find that the C atoms are no longer anions, but carries positive charges with values that range from +0.011 to +0.030 e. Since both the Li dopants and the carbon rings are positive under F = −0.010 au, it is obviously not beneficial to the H_2 storage. However, this should be a good result for the desorption process, since it weakens the binding between the H_2 and the storage material.

Fig. 2a gives the Mulliken charge results for all atoms in the cross section of the Li_8/SWCN storage material under F = +0.010 au. These results can be used to understand the entire charge redistribution of the system. In this Figure, it is readily seen that Li atoms possess different charge values depending on their positions. To explain this phenomenon, charge analysis was carried out for the surrounding six C atoms of each Li in the presence of a +0.010 au field. The results show that the hexagonal rings around Li(1) and Li(3) carry negative charges (−0.428 e for the former and −0.130 e for the latter), whereas the ones around Li(2) and Li(4) carry positive charges (+0.214 e for the former and +0.228 e for the latter). Correspondingly, Li(1) and Li(3) become cations whereas Li(2) and Li(4) are anions in order to maintain electrical balance. Under the positive field, the uppermost Li atoms transfer charges to the neighboring C atoms, and thus it is further ionized with net charge increase from +0.341 to +0.423 e. However, it seems that the charges will not just accumulate around these C atoms, but will go on moving downward from C labeled A to D. Thus, the Mulliken analysis

 This journal is © the Owner Societies 2009

View Article Online

Published on 17 August 2009. Downloaded on 7/6/2022 4:08:17 AM.

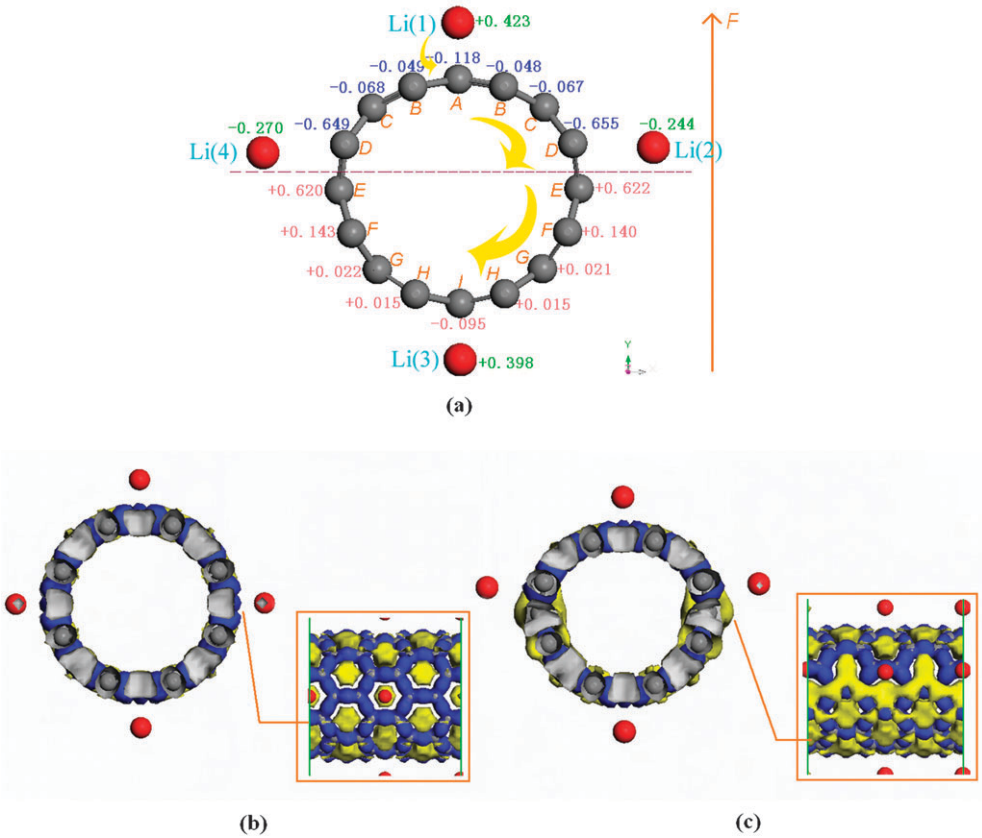

Fig. 2 Electronic analysis for the storage systems. (a) The Mulliken charge analysis for the atoms in the cross section of the Li_8/SWCN system under $F = +0.010$ au, where the unit of the atom charge is one electron charge e. (b) The plot of the electron density difference for the Li_8/SWCN system in the absence of field. (c) The plot of the electron density difference for the Li_8/SWCN system under $F = +0.010$ au. In plots b and c, the blue (or yellow) region shows where the electron density has been enriched (or depleted). The two insets show the side view.

shows that the entire C in the upper semicircle obtains electrons and thus is more negative. This leads to a heteropolar bonding between the SWCN and the Li dopants, and an extra dipole moment can be produced. This is consistent with the bonding mechanism suggested in prior studies.[7] On the contrary, the lower semicircle of the nanotube loses electrons and thus the most C atoms carry positive charges. In terms of the charge analysis results, the electrons will still transfer downward from E to I in this half circle. Thus, C atoms labeled E carried $+0.620\ e$ are the most positive. The charge values decrease gradually from $+0.620$, $+0.143$, $+0.022$, to $-0.095\ e$ for C atoms labeled E to I. This is not beneficial to the storage of the H_2 molecules, since the Li is now also a cation and can not induce an extra dipole moment between Li and C. Note that the lower part of the nanotube under the $F = +0.010$ au should be the same as the upper part of the nanotube under the $F = -0.010$ au. Therefore, Fig. 2a can also be used to illustrate the storage mechanism under negative fields.

The above results can also be visualized in the plots of electron density differences. Fig. 2b shows the charge variation without electric fields, where the blue area indicates where the electron has been enriched while the yellow one presents where the density has been depleted. Obviously, the C atoms gain while the Li dopants lose electrons under $F = 0.000$ au. This consists with the fact that the alkali metals would remain positively charged when doped on the SWCNs, not depending on their charge states or different carbon rings that they interact with.[55] However, when a positive field is introduced, as we have discussed above, the upper part of the SWCN gain electrons and appears blue, while the bottom part lose electrons and appears yellow, see Fig. 2c. The largest yellow and blue areas are around the C atoms labeled D and E in Fig. 2a.

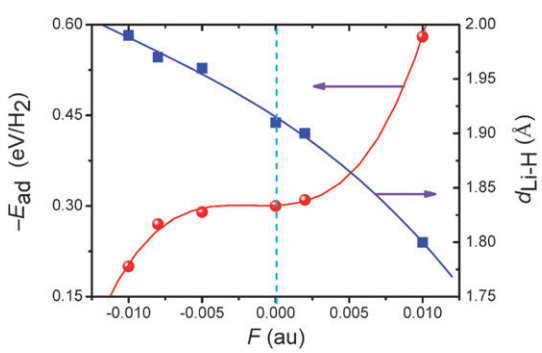

Fig. 3 Influences induced by the intensity of fields for the Bridge site of the H_2/Li_8/SWCN system. The plot shows the $-E_{ad}$ (indicated by the sphere line) and d_{Li-H} (indicated by the square line) values with respect to F where the discrete data are fitted by a third-order exponential function. When $F = 0.000$ au, the $-E_{ad}$ value of 0.30 eV/H_2 and d_{Li-H} value of 1.91 Å are selected as references.

View Article Online

Published on 17 August 2009. Downloaded on 7/6/2022 4:08:17 AM.

Fig. 3 provides the field intensity dependent results for the H_2/Li_8/SWCN system at the Bridge site, where E_{ad} = −0.58, −0.31, −0.30, −0.29, −0.27, and −0.20 eV/H_2 when F = +0.010, +0.002, 0.000, −0.005, −0.008, and −0.010 au, respectively. Thus, the binding strength is enhanced (or weakened) as the intensity of the positive (or negative) field increases. Although the trend is that as the field increases the binding becomes stronger, it is apparent that the F value cannot be infinitely large. In addition to the energy consumption, as F reaches 0.030 au the entire system was severely compressed along the direction of the field, and the excellent electronic properties of the Li-doped carbon nanotube would be degraded. Note that in this Figure, a plateau can be seen around $-0.005 < F < +0.002$ au in the $E_{ad}(F)$ curve. To understand why the E_{ad} values remain almost constant in such a large range, the Mulliken charge analysis was carried out for the systems under F = +0.002 and −0.005 au, and the obtained data are listed in Table 2. Under F = +0.002, E_{ad} is almost indeclinable compared with that under F = 0 where for instance there is no change for C(2), C(3), and C(6) atoms before adsorption while only 0.001 e variation is detected for the adsorbed H_2 molecule. These results suggest that the weak intensity cannot effectively "drive" the charge transfer within the system. On the other hand, although there is larger electronic redistribution occurs under F = −0.005 au, it is interesting to find that the C(1) and C(4) atoms carry negative charges, whereas the C(2), C(3), C(5), and C(6) carry positive ones, see Table 2. This is quite different from the case corresponding to F = −0.010 au, namely that all C atoms in the hexagon are completely positive, and thus render a significantly decrease in the H_2 binding strength. It is also different from those under F = +0.010 au that all the C atoms are negative, and thus a strong heteropolar bonding can be formed between SWCN and the Li dopant. Therefore, the F = −0.005 au here seems as a "transition state" during the charge redistribution process, and the influence of the field is "counteracted" by their own negative and positive C atoms to some extent. This is presumably the reason why the E_{ad} value is so "insensitive" to the F values in this range. Note that this insensitivity is relevant for practical applications since any small unexpected field fluctuation will not result in a state change (adsorption or desorption).

In addition to energy, some regularity induced by electric fields can also be observed in the geometric parameters for the H_2/Li_8/SWCN systems. As we can see in Fig. 3, d_{Li-H} = 1.80, 1.90, 1.91, 1.96, 1.97, and 1.99 Å when F = +0.010, +0.002, 0.000, −0.005, −0.008, and −0.010 au, respectively. Similarly, d_{Li-C}, and $Ø_x$ increase, while d_{H-H} and $Ø_y$ drop when a stronger intensity is introduced into the storage materials. This suggests that in addition to the direction, the intensity of the fields is also an efficient parameter to adjust the hydrogen storage.

Finally, to further understand the electronic hybridizations, the DOS plots are determined and shown in Fig. 4 for the H_2/Li_8/SWCN system. When F = 0.000 au, on the one hand, the main peak of Li-2s located at −9.40 eV hybridizes with the σ bonding of the H_2 molecule in the lower energy range, see Fig. 4a. On the other hand, the bands of Li interact with those of C at the higher energy range, where a sharp peak can be observed around −7.75 eV. This suggests that Li acts as a "bridge" in this reaction, which interacts with the molecule and the SWCN simultaneously. The peak around −2.06 eV corresponds to the hybridization of the Li-2s orbital with the π orbital of the SWCN, which is responsible for the bonding of the dopant to the nanotube.[22] It is known that all structures of SWCNs are made up of the sp^2 orbital of C atoms. After the Li and H_2 adsorptions, this orbital will change from the sp^2 to sp^3-like bonding, although the degree is not as large as that of the hydrogenation.[56,57] In addition, the chemisorbed Li atoms would partially donate their 2s valence electrons to the lowest conduction π* band of the SWCN, which binds H_2 in a molecular form due to the polarization mechanism.[58] Fig. 4b shows the bands interactions under F = +0.010 au, from which it is clear that although the orbitals under F = 0.000 and F = +0.010 au are quite similar, the former should be more stable since it has more evident peaks at the lower energy range. Comparing with Fig. 4a, the main peak of Li under fields moves toward the Fermi level and hybridizes with of the σ bonding of H_2 at −6.49 eV. Similarly, the π orbital of the SWCN varies from −2.06 to −0.90 eV under F = +0.010 au, and overlaps with the Li-2s orbital just below the Fermi level. Notably, the amount of C electrons near the Fermi level (around −5.00–0 eV) in Fig. 4a is much smaller than that in Fig. 4b, whereas larger than that under F = −0.010 au in Fig. 4c. These results may due to the fact that the C atoms obtain charges under the positive fields, whereas lose charges under the negative fields. In Fig. 4c, the orbitals of H, Li, and C interact tightly with each other at the lower energy range. In comparison with Fig. 4b, the bands of Li further move to the Fermi level and the sharpest peak hybridizes with H at −0.88 eV. In addition, the π orbital of the SWCN hybridizes simultaneously with the s orbitals of H and Li around −1.33 eV. These DOS changes confirm the strong effect of Li dopants in the hydrogen storage systems, even under electric fields.

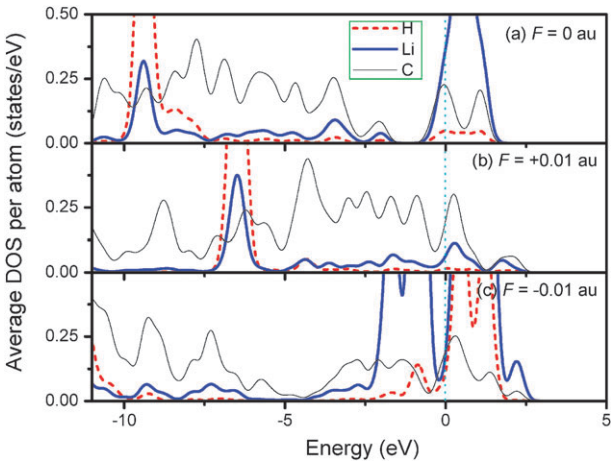

Fig. 4 The DOS plots under different fields. (a) F = 0.000 au, (b) F = +0.010 au, and (c) F = −0.010 au for the H_2/Li_8/SWCN system at the Bridge site. The Fermi level is set to zero and indicated by a dotted line.

In light of the above discussion, it is readily seen that the electric fields can be imposed to realize the ideal case for H_2 storage: increasing the bonding in the adsorption process and

 This journal is © the Owner Societies 2009

View Article Online

Published on 17 August 2009. Downloaded on 7/6/2022 4:08:17 AM.

decreasing it during the desorption one. Compared with other approaches, the fields have many advantages for practical applications, they are clean, easily acquirable, and adjustable in both direction and intensity. Although the carbon nanotube was selected as a prototype here, it is clear that this idea can be extended to other weak storage systems such as the graphene sheets. In addition, this idea may also be utilized to solve the releasing problem for the extremely strong binding systems, such as the Ti-doped nanostructures and the metal organic frameworks. In summary, our present work clearly demonstrates that the electric fields can be used as a useful reversible switch to control adsorption and desorption processes of H_2.

Conclusions

In conclusion, the DFT calculations with electric fields are employed to study the interactions between the H_2 molecules and the Li-doped SWCNs. For the Li_8/SWCN storage system, it was found that the E_{ad} at the Bridge site drops as high as -0.50 eV/H_2 under $F = +0.010$ au, whereas increases to -0.20 eV/H_2 under $F = -0.010$ au. These changes were interpreted by the results of charge analysis. The entire C atoms in the upper semicircle of SWCN obtains electrons and thus is more negative under the positive fields, which leads to a heteropolar bonding between the SWCN and the Li dopants, and an extra dipole moment can be produced. The opposite charge transfer depiction can be used to explain the binding mechanism under the negative fields. In addition, it is discernable that the binding strength increases (or decreases) as the enhancement of the positive (or negative) fields.

Acknowledgements

W. Liu and Q. Jiang acknowledge financial support from the National Key Basic Research and Development Program of China (Grant No. 2004CB619301). Y. H. Zhao, Y. Li, and E. J. Lavernia would like to acknowledge support by the Office of Naval Research of the USA (Grant No. N00014-08-1-0405) with Dr. Lawrence Kabacoff as program officer.

References

1 L. Schlapbach and A. Zuttel, *Nature*, 2001, **414**, 353–358.
2 A. S. Arico, P. Bruce, B. Scrosati, J. M. Tarascon and W. Van Schalkwijk, *Nat. Mater.*, 2005, **4**, 366–377.
3 R. H. Baughman, A. A. Zakhidov and W. A. de Heer, *Science*, 2002, **297**, 787–792.
4 C. Q. Sun, H. L. Bai, B. K. Tay, S. Li and E. Y. Jiang, *J. Phys. Chem. B*, 2003, **107**, 7544–7546.
5 S.-H. Jhi, *Phys. Rev. B: Condens. Matter Mater. Phys.*, 2006, **74**, 155424.
6 S. A. Shevlin and Z. X. Guo, *Appl. Phys. Lett.*, 2006, **89**, 153104.
7 S.-H. Jhi and Y.-K. Kwon, *Phys. Rev. B: Condens. Matter Mater. Phys.*, 2004, **69**, 245407.
8 Q. Sun, P. Jena, Q. Wang and M. Marquez, *J. Am. Chem. Soc.*, 2006, **128**, 9741–9745.
9 G. E. Froudakis, *Nano Lett.*, 2001, **1**, 531–533.
10 I. Cabria, M. J. López and J. A. Alonso, *J. Chem. Phys.*, 2005, **123**, 204721.
11 S.-H. Jhi, *Catal. Today*, 2007, **120**, 383–388.
12 X. J. Wu, Y. Gao and X. C. Zeng, *J. Phys. Chem. C*, 2008, **112**, 8458–8463.
13 L. Chen, Y. Zhang, N. Koratkar, P. Jena and S. K. Nayak, *Phys. Rev. B: Condens. Matter Mater. Phys.*, 2008, **77**, 033405.
14 C. Liu, Y. Y. Fan, M. Liu, H. T. Cong, H. M. Cheng and M. S. Dresselhaus, *Science*, 1999, **286**, 1127–1129.
15 O. V. Pupysheva, A. A. Farajian and B. I. Yakobson, *Nano Lett.*, 2008, **8**, 767–774.
16 K. R. S. Chandrakumar and S. K. Ghosh, *Nano Lett.*, 2008, **8**, 13–19.
17 M. I. Rojas and E. P. M. Leiva, *Phys. Rev. B: Condens. Matter Mater. Phys.*, 2007, **76**, 155415.
18 E. Klontzas, A. Mavrandonakis, E. Tylianakis and G. E. Froudakis, *Nano Lett.*, 2008, **8**, 1572–1576.
19 B. Liu, Q. Y. Yang, C. Y. Xue, C. L. Zhong and B. Smit, *Phys. Chem. Chem. Phys.*, 2008, **10**, 3244–3249.
20 E. Klontzas, E. Tylianakis and G. E. Froudakis, *J. Phys. Chem. C*, 2008, **112**, 9095–9098.
21 P. Chen, X. Wu, J. Lin and K. L. Tan, *Science*, 1999, **285**, 91–93.
22 T. Yildirim and S. Ciraci, *Phys. Rev. Lett.*, 2005, **94**, 175501.
23 X. J. Wu, J. L. Yang and X. C. Zeng, *J. Chem. Phys.*, 2006, **125**, 044704.
24 M. Yoon, S. Y. Yang, C. Hicke, E. Wang, D. Geohegan and Z. Y. Zhang, *Phys. Rev. Lett.*, 2008, **100**, 206806.
25 S. Meng, E. Kaxiras and Z. Y. Zhang, *Nano Lett.*, 2007, **7**, 663–667.
26 H. Pan, Y. P. Feng and J. Y. Lin, *Appl. Phys. Lett.*, 2007, **90**, 223104.
27 B. K. Rao and P. Jena, *Europhys. Lett.*, 1992, **20**, 307–312.
28 C. H. Ahn, A. Bhattacharya, M. Di Ventra, J. N. Eckstein, C. D. Frisbie, M. E. Gershenson, A. M. Goldman, I. H. Inoue, J. Mannhart, A. J. Millis, A. F. Morpurgo, D. Natelson and J. M. Triscone, *Rev. Mod. Phys.*, 2006, **78**, 1185–1212.
29 L. Qiao, W. T. Zheng, Q. B. Wen and Q. Jiang, *Nanotechnology*, 2007, **18**, 155707.
30 M. Tomonari and O. Sugino, *Chem. Phys. Lett.*, 2007, **437**, 170–175.
31 A. Migani, C. Sousa, F. Sanz and F. Illas, *Phys. Chem. Chem. Phys.*, 2005, **7**, 3353–3358.
32 J. Zhou, Q. Wang, Q. Sun, P. Jena and X. S. Chen, http://arxiv.org/ftp/arxiv/papers/0903/0903.3079.pdf.
33 W. Liu, Y. H. Zhao, Y. Li, Q. Jiang and E. J. Lavernia, *J. Phys. Chem. C*, 2009, **113**, 2028–2033.
34 B. Delley, *J. Chem. Phys.*, 1990, **92**, 508–517.
35 B. Delley, *J. Chem. Phys.*, 2000, **113**, 7756–7764.
36 M. Cobian and J. Iniguez, *J. Phys.: Condens. Matter*, 2008, **20**, 285212.
37 C. Ataca, E. Aktürk, S. Ciraci and H. Ustunel, *Appl. Phys. Lett.*, 2008, **93**, 043123.
38 P. L. de Andres, R. Ramírez and J. A. Vergés, *Phys. Rev. B: Condens. Matter Mater. Phys.*, 2008, **77**, 045403.
39 J. Zhao, A. Buldum, J. Han and J. P. Lu, *Phys. Rev. Lett.*, 2000, **85**, 1706–1709.
40 A. Nikitin, X. L. Li, Z. Y. Zhang, H. Ogasawara, H. J. Dai and A. Nilsson, *Nano Lett.*, 2008, **8**, 162–167.
41 M. Yoon, S. Y. Yang, E. Wang and Z. Y. Zhang, *Nano Lett.*, 2007, **7**, 2578–2583.
42 Y. V. Shtogun and L. M. Woods, *J. Phys. Chem. C*, 2009, **113**, 4792–4796.
43 J. P. Perdew and Y. Wang, *Phys. Rev. B: Condens. Matter Mater. Phys.*, 1992, **45**, 13244–13249.
44 B. Delley, *Modern Density Functional Theory: A Tool for Chemistry*, ed. J. M. Seminario and P. Politzer, *Theoretical and Computational Chemistry*, Elsevier Science, Amsterdam, 1995, vol. 2.
45 S. González, C. Sousa and F. Illas, *Surf. Sci.*, 2004, **548**, 209–219.
46 K. P. Huber and G. Herzberg, *Molecular Spectra and Molecular Structure. IV. Constants of Diatomic Molecules*, Van Nostrand, New York, 1979.
47 J. Li, T. Furuta, H. Goto, T. Ohashi, Y. Fujiwara and S. Yip, *J. Chem. Phys.*, 2003, **119**, 2376–2385.

View Article Online

48 O. Gülseren, T. Yildirim and S. Ciraci, *Phys. Rev. Lett.*, 2001, **87**, 116802.
49 T. Yildirim, J. Iniguez and S. Ciraci, *Phys. Rev. B: Condens. Matter Mater. Phys.*, 2005, **72**, 153403.
50 G. H. Gao, T. Çağin and W. A. Goddard, *Phys. Rev. Lett.*, 1998, **80**, 5556–5559.
51 P. O. Krasnov, F. Ding, A. K. Singh and B. I. Yakobson, *J. Phys. Chem. C*, 2007, **111**, 17977–17980.
52 W.-Q. Deng, X. Xu and W. A. Goddard, *Phys. Rev. Lett.*, 2004, **92**, 166103.
53 F. Illas, F. Mele, D. Curulla, A. Clotet and J. M. Ricart, *Electrochim. Acta*, 1998, **44**, 1213.
54 Z. M. Ao, W. T. Zheng and Q. Jiang, *Nanotechnology*, 2008, **19**, 275710.
55 G. Mpourmpakis and G. Froudakis, *J. Chem. Phys.*, 2006, **125**, 204707.
56 A. Tokura, F. Maeda, Y. Teraoka, A. Yoshigoe, D. Takagi, Y. Homma, Y. Watanabe and Y. Kobayashi, *Carbon*, 2008, **46**, 1903–1908.
57 G. Y. Zhang, P. F. Qi, X. R. Wang, Y. R. Lu, D. Mann, X. L. Li and H. J. Dai, *J. Am. Chem. Soc.*, 2006, **128**, 6026–6027.
58 S. Dag, Y. Ozturk, S. Ciraci and T. Yildirim, *Phys. Rev. B: Condens. Matter Mater. Phys.*, 2005, **72**, 155404.

Published on 17 August 2009. Downloaded on 7/6/2022 4:08:17 AM.

This journal is © the Owner Societies 2009